Graphene Based Sensors for Air Quality Monitoring – Preliminary Development Evaluation

Denise Machado[1,2], Maria J. Hortigüela[1], Gonzalo Otero-Irurueta[1], Paula A.A.P. Marques[1], Ricardo Silva[2], Rui F. Silva[2] and Victor Neto[1,*]

[1]Centre for Mechanical Technology and Automation (TEMA), Department of Mechanical engineering, University of Aveiro, 3810-193 Aveiro, Portugal

[2]Aveiro Institute of Materials (CICECO), Department of Materials and Ceramic Engineering, University of Aveiro, 3810-193 Aveiro, Portugal

Abstract: Indoor air pollution can induce adverse health effects on building occupants and pose a significant role in health worldwide. To avoid such effects, it is extremely important to monitor and control common indoor pollutants such as CO_2, VOCs and relative humidity. Therefore, this work focuses on recent advances in the field of graphene-based gas sensors, emphasizing the use of modified graphene that broadly expands the range of nanomaterials sensors. Graphene films were grown on copper by chemical vapor deposition (CVD) and transferred to arbitrary substrates. After synthesis, the samples were functionalized with Al_2O_3 by ALD and characterized by a large set of experimental techniques such as XPS, Raman and SEM. The results demonstrated that graphene was successfully synthesized and transferred to SiO_2, glass and polymer. As a proof-of-concept, ALD of Al_2O_3 was performed on the graphene surface to produce a graphene/metal oxide nanostructure towards the development of nanocomposites for gas sensing. From this perspective, a laboratory prototype device based in measuring the electrical properties of the graphene sample as a function of the gas absorption is under development.

INTRODUCTION

Volatile organic compounds (VOCs), particulates (PM) of diverse sizes and microbial contaminants deteriorate indoor air quality (IAQ) and have subsequent effects on human health [1]. According to World Health Organization (WHO), it is estimated that, in 2016, household air pollution is estimated to have caused 3.8 million deaths from non-communicable diseases (including heart disease, stroke and cancer) and acute lower respiratory infections. In the same year, in Portugal, the mortality rate attributed to household and ambient air pollution was 9,8 per 100 000 population [2]. For all these reasons, there is a need to control air quality so that the values do not exceed the limits imposed by the European Commission [3].

In the last years, devices that can measure and monitoring chemical-, physical- and biological- changes in the environment, with low cost, compact size, and low-power consumption have been developed under the form of sensors [4, 5]. Sensors are devices that provides an output signal usable in response to a specific measure, such as observable chemical reactions between certain materials [6]. A gas sensor can be used to monitor potentially dangerous leaks and, if connected to an automatic control system, can be an advantage in detecting high concentrations of gas in a given environment [7, 8].

These can be classified according to their operating principle, namely metal-oxide semiconductor sensors (MOS) based on conductivity variation [9], amperometric sensors based on solids or liquid electrolytes [10], or optical sensors using fluorescence or absorption of light [11]. Metal oxides have been fabricated to monitor and detect VOCs for more than 50 years due to their semiconducting properties. Semiconducting metal oxides (SMOXs) are attractive for gas sensing applications since they are cheap, flexible to apply to different manufacturing methods and easy to use [12, 13].

They may also be divided into specifics sensors, which provide specific information regarding a target compound, or, non-specific, that provide a global response to one or several families of chemical species (In section 3 the sensors for air

*Centre for Mechanical Technology and Automation (TEMA), Department of Mechanical engineering, University of Aveiro, 3810-193 Aveiro, Portugal; E-mail: vneto@ua.pt

monitoring are presented in more detail) [14]. They play an important role in various fields of application such as environmental monitoring, industrial production and safety, and when integrated into measurement systems, they can detect changes that occur in the physical environment [14, 15].

Thus, due to its unique structure, uncommon chemical and physical properties, good conductivity and large specific surface area graphene based sensors performed well with good accuracy, rapidness, high sensitivity and selectivity, low detection limits, and long term stability [16]. Nowadays, it is clear that graphene is a very promising candidate to integrate sensors for IAQ monitoring [17, 18]. However, pristine graphene is chemically inert to be useful in the detection of gases. As such, an approach to increase its chemical activity is required, through functionalization [19].

The present work focuses on recent advances in the field of graphene-based gas sensors, emphasizing the use of modified graphene that broadly expands the range of nanomaterials sensors and intends to be the starting point for the development of a functional prototype of the chemical gas sensor with high sensitivity, from the modified graphene structures.

Air Quality Requirements, Parameters and Assessment

Indoor air pollutants may originate from a different range of sources such as combustion for heating, material deterioration and VOCs emitted from paints, varnishes and preservatives. In addition, insoluble nanoparticles as well as biological particles present in indoor air, can also affect human health through direct toxicity, immune and infectious mechanisms [20-30].

For air quality assessment, numerous indices were proposed. The first index was the "Pollutant Standard Index" (PSI), which was modified and replaced by the "Air Quality Index" (AQI), both of which were developed and introduced by the United States Environmental Protection Agency (US-EPA) [24]. In Europe, the Environment Directorate General of The European Commission ("DG Environment") has developed a legislation, which establishes health-based standards and objectives for a number of pollutants present in the air. These standards and objectives are summarized in the Table **1** [3]. As people spend a substantial part of their time on buildings, maintaining indoor air quality levels becomes a challenge to overcome. Thus, the use of sensors and the development of new materials, such as graphene-based sensors, allow these levels to be monitored and controlled.

Conventional analytical instruments can be use accurately to measure the concentration of pollutants inside the buildings, but are not practical because of their complexity, volume and emitted noise. In addition, most analyzes require sample preparation, so a real-time analysis is difficult to obtain [21, 25, 26]. Solid-state chemical sensors have been widely used, however, also their measurement accuracy is limited and

Table 1: **Target and Limit Values for the Parameters of Indoor Air [3]**

Pollutant	Concentration	Averaging period	Legal nature
$PM_{2.5}$	25 µg/m^3	1 year	Target value to be met as of 1.1.2010
			Limit value to be met as of 1.1.2015
SO_2	350 µg/m^3 125 µg/m^3	1 hour 24 hours	Limit value to be met as of 1.1.2005 Limit value to be met as of 1.1.2005
NO_2	200 µg/m^3 40 µg/m^3	1 hour 1 year	Limit value to be met as of 1.1.2010 Limit value to be met as of 1.1.2010
PM_{10}	50 µg/m^3 40 µg/m^3	24 hours 1 year	Limit value to be met as of 1.1.2005 Limit value to be met as of 1.1.2005
Pb	0.5 µg/m^3	1 year	Limit value to be met as of 1.1.2005 (or 1.1.2010 in the immediate vicinity of specific, notified industrial sources; and a 1.0 µg/m^3 limit value applied from 1.1.2005 to 31.12.2009)
CO	10 µg/m^3	Maximum daily 8 hours mean	Limit value to be met as of 1.1.2005
Benzene	5 µg/m^3	1 year	Limit value to be met as of 1.1.2010
Ozone	120 µg/m^3	Maximum daily 8 hour mean	Target value to be met as of 1.1.2010
As	6 ng/m^3	1 year	Target value to be met as of 31.12.2012
Cd	5 ng/m^3	1 year	Target value to be met as of 31.12.2012
Ni	20 ng/m^3	1 year	Target value to be met as of 31.12.2012
Polycyclic Aromatic Hydrocarbons	1 ng/m^3 (expressed as concentration of Benzo(a)pyrene)	1 year	Target value to be met as of 31.12.2012

present a long-term stability problem [26]. Nanotechnology becomes to fill existing flaws by providing numerous opportunities for the development of the next generation gas detector with enhanced sensor performance such as high specificity, fast response, ultra-high sensitivity at extremely low concentrations and coverage, low power consumption, room temperature operation and good reversibility [26, 27].

Graphene as a Sensor Device

In the recent years, there has been a significant improvement in the construction of sensors with the incorporation of several nanomaterials, such as nanowires synthesized from metals, metal oxides, semiconductors, carbon nanotubes (CNT) and metal nanoparticles. Due to their conductive properties and high surface-to-volume ratio, nanomaterial thus contributing to the improvement of the analytical performance of such sensors [28-30]. One of the advantages of semiconductor gas sensors is the ability of easily combining the functions of a sensitive element and signal converter and control electronics in the same device, greatly simplifying the design [26, 31]. Nanostructures have a high surface-to-volume ratio, which is one of the most important characteristics of a material to be used for gas sensing and provides large active surface area for the interaction of gas molecules. This strongly favors the adsorption of gases on nanostructures and leads to highly sensitive sensors performance [32]. The most recent example of the application of new materials in this type of sensors are the studies of the use of graphene in sensors for air quality measurement [33, 34]. The two-dimensional (2D) materials have captured

enormous interest after the first successful isolation of graphene in 2004 [28].

Graphene is an extremely diversified material, with exceptional characteristics that allows producing different materials with varied properties, leading to great technological advances in the most varied areas [16, 35]. Because silicon-based technology is close to the limit in terms of performance improvement, the electronic properties of graphene make it an excellent choice for the semiconductor industry [33, 36].

Compared to other materials graphene showed great potential for the construction of sensors. The combination of extraordinary properties makes graphene highly sensitive to changes of local environmental conditions, which is an important advantage in the sensing field, since all carbon atoms interact directly with the analyses, thus promoting higher sensitivity [34, 37]. Fluctuations due to thermal movement of charges and defects limits the sensitivity of graphene. Each atom in the graphene is exposed to its environment, allowing it to sense individual events when a gas molecule attaches to graphene's surface [38]. The adsorbed molecules change the concentration in graphene, which leads to changes in resistance. The achieved sensitivity is due to the fact that graphene is an electronically low-noise material, which makes it a promising candidate for gas sensors [39].

The synthesis of graphene can be divided into two main categories: physical- and chemical methods as shown in

Table 2:   Comparisons on Different Aspects of Methods for Graphene Synthesis [42]

Synthesis methods	Precursors	Layer characters	Advantages	Disadvantages
Micromechanical exfoliation	Graphite	Single and multiple layers; dimension ca. 10 μm	Simplicity; high quality; low cost	Time-consuming; low yields
Chemical vapor deposition	Hydrocarbon gases	Single and multiple layers; dimension ca. 100 μm	High quality; uniform; largescale production	High temperature (1000°C); high cost; complicated process; low yields
Epitaxial growth on silicon Carbide	SiC wafer	Single and multiple layers; dimension ca. 50 μm	Uniform; high quality	High cost; low yields; high temperature; high vacuum; single-crystal substrate
Arc discharge	Graphite	Single and multiple layers; dimension hundreds of nm ca. 10 μm	Low cost; easy doping; good crystallinity; high thermal stability	Non-uniform; impure
Chemical reduction of GO	Graphite	Single and multiple layers; dimension tens of nm to ca. 100 μm	High yields; low cost; largescale production	Low quality
Intercalation of small molecules within graphite	Graphite	Single and multiple layers; dimension in tens of μm	Simplicity; benign; large-scale production; low-cost	Time-consuming; impure
Unzipping CNTs	CNTs	Single and multiple layers; dimension in several μm	Low cost; large-scale production; high quality (plasma etching)	Time-consuming; complicated process
Electrochemical method	Graphite	Single and multiple dimension; hundreds of nm to ca. 10 μm	Low cost; high quality	Low yields
Total organic synthesis	PAHs	Single layer, dimension less than 20 nm	High quality precisely defined structures	High cost; limited size range; complicated process

Table **2** and depends, among others, on the crystallinity, purity and desired size [40, 41].

The chemical vapor deposition (CVD) process is the most common method to grow graphene. It consists of breaking the bonds of the molecules of a gas subjected to high temperatures, so that the atoms coming from the gas are deposited on a certain substrate and the graphene films synthesized by this method can be transferred to other substrates, facilitating their integration into various materials [30, 43].

The deposition of high-quality graphene from CVD process is usually done onto various transition-metal substrates with copper (Cu) as the most popular metal to produce homogeneous single layer graphene in large-area [44-46]. Copper is one of the best catalyst options because, even at 1000°C, the solubility of carbon in copper is insignificant, so the carbon precursor forms graphene directly on copper surface during the growth step [47, 48].

Functionalization of Graphene by Atomic Layer Deposition (ALD)

The operating principle of graphene devices is similar to other solid-state sensors and is based on changes in their electrical conductivity due to gas molecules adsorbed on their surface, acting as donors or receivers [49, 50]. Depending on the size relationship between a chemical species and material, these interfaces may be superficial when chemical and/or physical adsorption occurs, or volume interactions, when the chemical absorption passes through the active layer of the sensor (bulk effect) [51].

Figure **1** represents the schematic diagram of a back-gated graphene device on top of an arbitrary substrate during NH_3 exposure with also a representation of current-biased measurement setup [51].

The natural properties of graphene and functionalized graphene, such as massless charged carriers, and the high interaction with gas molecules, make these one of the most efficient materials for detecting gases. The type of interactions between atoms and molecules of graphene differ from the weak interactions of van der Waals with the strong covalent bonds, which leads to an intense change in the conductivity of the graphene [39, 52, 53].

Due to its high-quality crystal lattice, graphene has intrinsically low electrical noise and is capable of transmitting more charge fluctuations. Consequently, some additional electrons can create a noticeable change in the conductance of graphene. As all carbon atoms are located on the surface, small changes in the resistance of a graphene sheet, even if down the molecular level, are measurable [54] making graphene highly sensitive to any change in its surrounding environment [39,52].

One of the techniques that allow the manufacture of atomic-scale materials and components either as thin film or as nanoparticles with accuracy that cannot be achieved by current CVD techniques is atomic layer deposition (ALD). As matter of fact, ALD has proved to be a technique of choice for the coating of nanostructured carbon materials and it's based on self-limiting surface reactions separated in gas phases [55, 56]. When two precursors A and B react on gas phases during the CVD deposition to produce a thin film on the surface of the substrate, the same precursors react separately in ALD with the substrate surface to produce a uniform coating. The principle is based on the splitting of the deposition reaction in two separated self-limiting reactions due to the deposition mechanism [57].

ALD of aluminum oxide (Al_2O_3) using trimethylaluminum (TMA) and water as precursor were developed as a model for ALD system. The surface reaction during the ALD deposition mechanism has one of the highest ALD reaction enthalpies [57, 58].

Nowadays, with the down-scaling of semiconductor device dimensions, the requirement of nanotechnology has grown enormously and ALD has found new opportunities in microelectronics industry for the development of metal oxide semiconductor field effect transistors (MOSFETs) and high-density memory devices with high-level integration [59, 60]. In this way, ALD has proved to be suitable for the deposition of metal oxides. In general, metal oxide semiconductors are used as active layers in resistive sensors [61, 62].
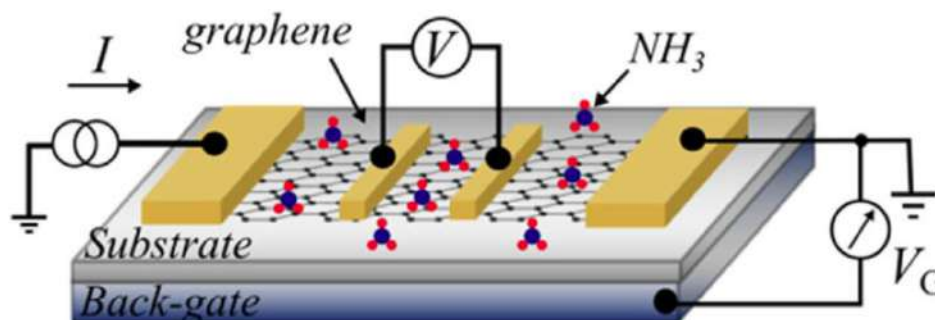
Figure 1: Schematic of a back-gated graphene device. [Reproduced with permission from ref [51], copyright @elsevier].

Authors: Cadore AR, Mania E, Alencar AB, *et al*.

As a proof-of-concept, we synthesized CVD graphene on copper foils, in order to fabricate the platform for the sensing devices. The functionalization of CVD graphene via ALD is an interesting way to modify the surface properties of the as-prepared graphene. As result, a nanostructure composed of graphene/metal oxide is obtained for detecting various gas species at room temperature.

EXPERIMENTAL

Synthesis of Graphene by CVD

Graphene samples were synthesized using CVD method at 950 °C and at a pressure of 4,67 $\times$ 10^4 Pa. Copper with 25µm thickness was used as catalytic substrate. The heating step was started by increasing the furnace temperature from room temperature ($\approx$ 20 °C) to 950 °C under 117 sccm (standard cubic centimeters per minute) N_2 and 27 sccm H_2 atmosphere. The annealing process was carried out under same conditions to remove oxide from the copper foil and to increase the grain size of Cu. After keeping temperature at 950 °C for 64 min, it was used an atmosphere rich in methane at a flow rate of 16 sccm in order to grow graphene for 5 min and, finally, the sample was cooled down at natural velocity. The experimental parameters (temperature profile, gas composition and time) are shown in Figure **2**.

Transfer Process of Graphene

Graphene films were removed from the copper foils by etching in a solution of iron chloride III ($FeCl_3$) with deionized water, as shown in Figure 3. Once the copper oxidation is complete, it is necessary to remove the floating graphene membrane so that it is subsequently transferred to an arbitrary substrate. The suspended films were transferred to deionized water (about 2 min) to remove any residual copper etchant. Afterwards the graphene was transferred for SiO_2/Si

(Figure **3.1**), glass (Figure **3.2**) and polymer (Figure **3.3**). From Figure **3** it is also possible to notice that the graphene was successfully removed from the copper foils and it can be seen as grey contrast on the top of the glass, for example (Figure **3.2**). This transfer step is crucial, concerning the integration of the graphene in the sensor device fabrication process.

ALD of Al_2O_3

After the transfer step, the graphene functionalization was done with Al_2O_3 coating by ALD in home-made cross-flow reactor using a stop valve feature. ALD of Al_2O_3 process is based on the reaction between the water (H_2O) and trimethylaluminum (TMA) precursors at 100°C. To this end, the TMA and H_2O were alternately pulsed on the graphene surface during deposition and the growth relies on two self-limiting surface reactions. Both precursors were kept at room-temperature and pure nitrogen (N_2) was used as carrier and purge gas. To ensure higher exposure time of precursor gas over the graphene surface network, the stop valve mode was used. Several samples were prepared, with different number of ALD cycles.

The as-prepared nanostructures were characterized by a large set of experimental techniques such XPS, Raman, and SEM. In particular, the Raman scattering spectroscopy is remaining as a major technique in the study of graphene, providing a quick and simple characterization of the graphene structural defects accordingly to the literature [63]. SEM micrographs were obtained on a TM4000Plus microscope (Hitachi). The micrographs were recorder by a backscatter electrons detector for high contrast. Micro-Raman spectroscopy was performed using a Jobin Yvon (HORIBA) HR800 instrument, using a 530 nm laser wavelength as excitation source (Kimmon, IK series, Japan) and x100 objective (NA=0.9, Olympus, Japan).
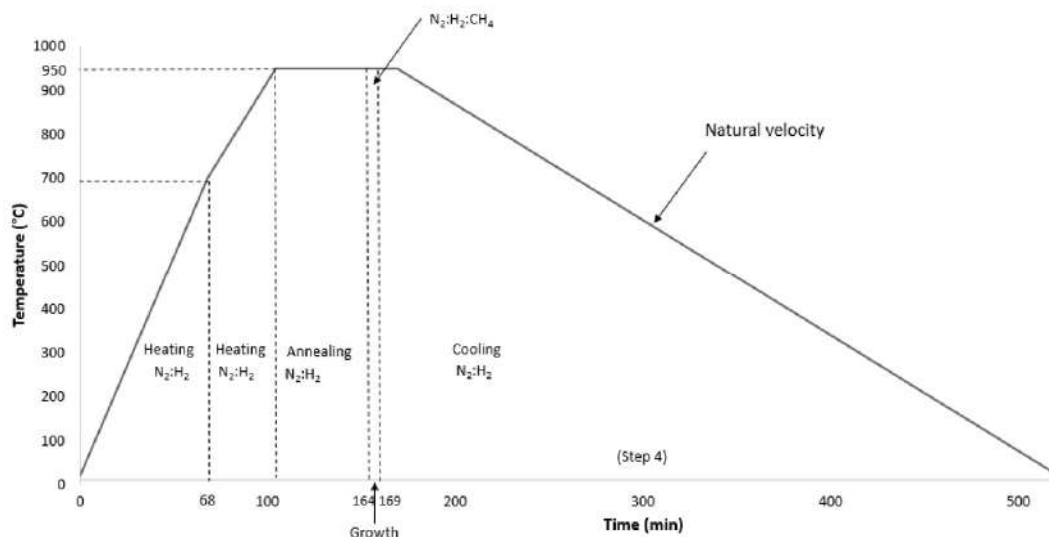
Figure 2: Optimized protocol of growth of graphene by CVD.

Authors: Denise Machado, Maria J. Hortigüela and Gonzalo Otero-Irurueta.
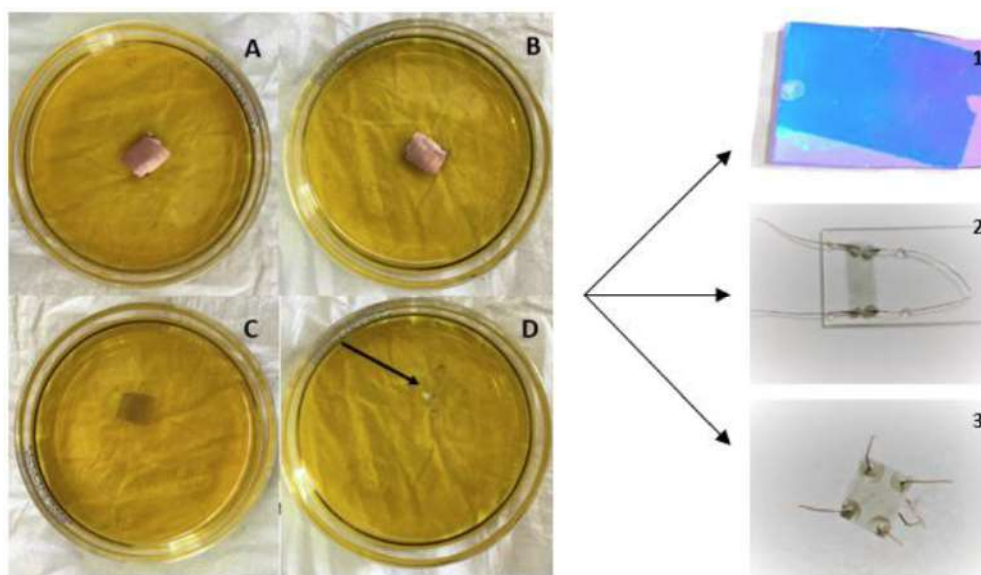
Figure 3: Transfer process of the graphene (from **A** to **D**) to: 1) SiO$_2$/Si, 2) glass, 3) polymer.

Authors: Denise Machado, Maria J. Hortigüela and Gonzalo Otero-Irurueta.

High resolution X-ray photoelectron spectroscopy (XPS) was recorded in an ultra-high vacuum system (base pressure of 200 Pa). The system combines a hemi-spherical electron energy analyzer (SPECS Phoibos 150), a delay-line detector and a monochromatic Al Kα X-ray source (1486,74 eV). The spectra were acquired at normal emission take-off angle and with a pass-energy of 20 eV.

RESULTS AND DISCUSSION

In Figure **4**, it is possible to observe the differences between the Raman spectra of the as-prepared graphene (red line) and the functionalized graphene after 50 ALD cycles of Al$_2$O$_3$ (green line). Three important features were observed in the Raman spectra and they are common to both samples; D-band (around 1300 cm^{-1}) is usually associated with the density of defects present in the graphene network, that is, the intensity of the D band is directly related to the concentration of defects. On the other hand, the G-band (around 1580 cm^{-1}) is associated to the in-plane vibration of the sp^2 carbon atoms. Finally the 2D-band (around 2700 cm^{-1}) results from a second-order process [41]. These results indicate high-quality graphene grown on Cu emphasized by the less pronounced presence of the D band when compared with the other two bands (G and 2D bands). Most importantly, the ALD of Al$_2$O$_3$ does not affect the intrinsic properties of the graphene demonstrated by the similarities of the Raman measurements. This finding also suggests that the ALD is a non-destructive technique to functionalize this type of nanomaterials.

These modes are present in all graphene-based materials, however, their frequencies, intensities, and line widths are influenced by other factors, such as the number of graphene layers, extern doping or laser excitation energy.
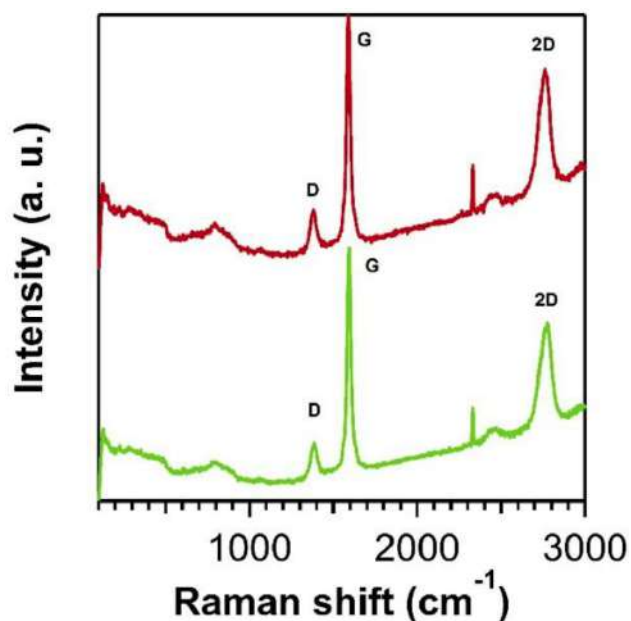
Figure 4: Raman spectra of the as-prepared graphene (red line) and after 50 ALD cycles with Al$_2$O$_3$ (green line). The Raman spectra was acquired at different points of the samples.

Author: Ricardo Silva.

XPS is a well-established experimental technique to understand the elemental composition and the chemical environment of the detected elements on surfaces. Figure **5A-B** shows the comparison among high-resolution spectra of as grown (top) and transferred graphene (down), as it (red) and after Al$_2$O$_3$ functionalization by ALD (black). All the C 1s spectra present asymmetric sharp peaks typical of graphene. The full width at half maximum (FWHM) of C 1s from Gr on Cu and Gr transferred onto SiO$_2$ have quite low values, 0,61 eV and 0,64 eV, respectively. This fact besides the absence
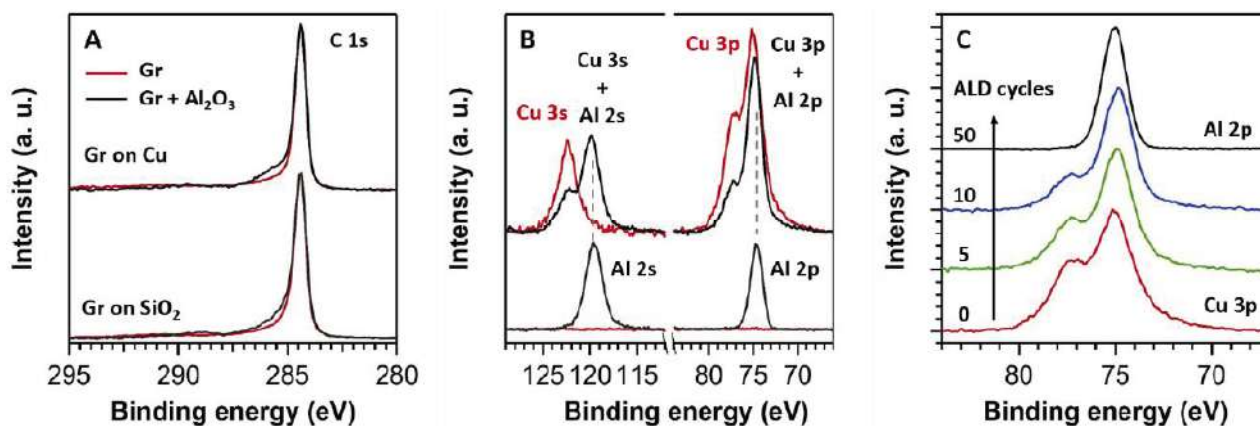
Figure 5: XPS spectra: **A**) normalized C1s peak, **B**) Al2s/Cu3s and Al2p/Cu3p, from Gr on Cu (top) and Gr transferred to SiO$_2$ (down) samples, as it (red) and after Al$_2$O$_3$ deposition by 10 cycles of ALD (black), **C**) Al2p/Cu3p region as a function of ALD cycles.

Authors: Maria J. Hortigüela and Gonzalo Otero-Irurueta.

of peaks at BEs related to carbon-oxygen species indicate a good quality sp^2 carbon and a low damage of the structure due to the transfer process. After ALD functionalization FWHM of C 1s peaks (black drawn) increase slightly, 0,63 eV on Cu and 0,69 eV on SiO$_2$, and it appears a small shoulder at higher BE due to adventitious carbon contamination, more easily attached to Al$_2$O$_3$ than to Gr.

Figure **5B** shows the energy regions corresponding to Al 2p and Al 2s before (red) and after (black) 10 cycles of ALD functionalization. In the case of Gr on SiO$_2$ (down) symmetric peaks show up centered at 74,6 eV and 119,6 eV confirming the successful deposition of aluminum oxide [64]. The case of Gr on Cu (top) is not so obvious due to the overlapping of Al 2s and Al 2p with Cu 3s and Cu 3p regions, respectively. Anyway, it is clear that the intensity of the component at the BE position of Al increase while the intensity coming from Cu peaks decrease.

ALD technique allows the control over the coverage of the sample. As it can be seen in Figure **5C**, the increment of ALD

cycles increase progressively the coverage with aluminum oxide until a point (50 cycles) at which the Cu substrate cannot be detected by XPS.

Figure **6A-B** shows the difference between SEM performed on graphene sample and on SiO$_2$/Si with a growth time of 5 min. In Figure **6A** can notice that the graphene film (darker contrast) are continuous, uniform and clean without noticeable particles, but grain boundaries, Cu surface steps, and wrinkles are observed. Figure **6B** shows that the graphene sheet has a much rougher surface, with some impurities and cracks. This roughness contrast can be explained as the topographic contrast that is the most frequent application of the SEM.

The results clearly demonstrate that graphene was successfully synthesized and transferred to the substrate.

Accordingly to the XPS studies, Al$_2$O$_3$ was successfully deposited on the graphene surface demonstrating the following two features: i) the graphene 2D nanomaterial is a suitable platform for the elaboration of nanostructures
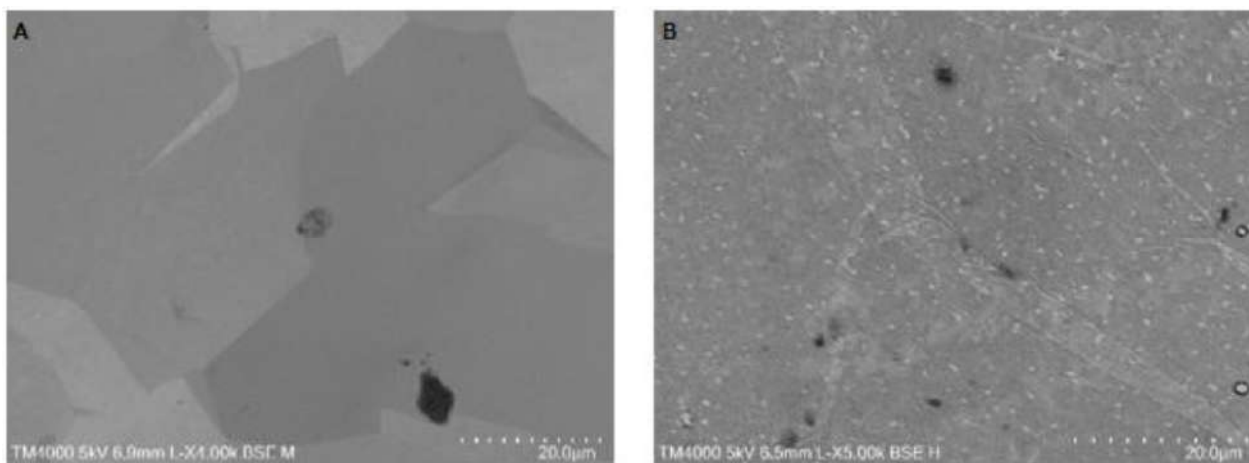
Figure 6: SEM image: **A**) Graphene in copper, **B**) Graphene transferred to SiO$_2$/Si.

Authors: Denise Machado, Maria J. Hortigüela and Gonzalo Otero-Irurueta.
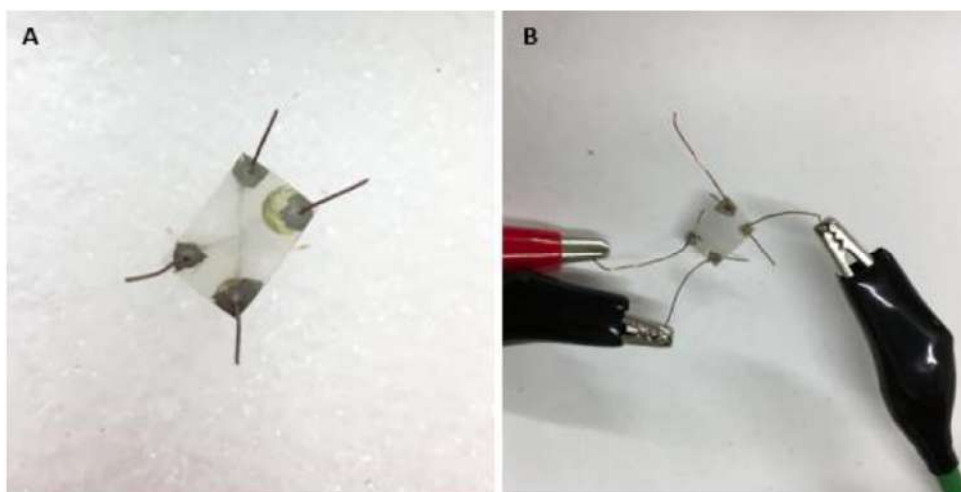
Figure 7: A) Experimental device, **B**) the connection with three cables for the graphene sensor.

Authors: Maria J. Hortigüela and Gonzalo Otero-Irurueta.

comprised of graphene/metal oxide and ii) the ALD technique is a non-destructive approach for the graphene surface functionalization. The combination of these features provides the means to develop new nanocomposites for gas sensing applications.

From this perspective, a laboratory prototype device based on measuring electrical properties of the graphene sample as a function of the gas absorption is under development. The basic concept to create a system using a graphene layer to detect the presence of gases in the atmosphere is based on the fact that the graphene surface can absorb these gases and the gas particles will change its resistivity value. The first step was to create a suitable device to measure the resistance and its variation in a graphene layer. This must be cheap, affordable, easy to replicate and a flexible measuring system that can guarantee a good accuracy and low noise levels. Figures **7A** shows our experimental device and **7B** the connections with three cables for the graphene sensor to detect CO_2 in the atmosphere. In order to create a sensor, it

is important to supply the graphene layer with very low currents and voltages to avoid burning or damaging the sensor.

The measuring system (Figure **8**) consists of a chip-board to provide the desired current and voltage signal, and hardware to connect the I/O of the board with the graphene sensor. The board chosen is a Cypress CY8CKIT-059 PSoC® 5LP that has been programmed using the PSOC Creator 4.2 software. To reduce the noise, a real low-pass filter was built in the electric circuit on the bread-board, connecting a capacitor between the voltage output of the sensor and the ground. A led was also added in the circuit to signal the presence of CO_2 in case the resistance value was going under a minimum threshold.

The possible solutions initially considered for the measurement hardware system were a four-points probe and a Wheatstone bridge architecture. The four-points probe is commonly used to measure sheet resistance of thin films,
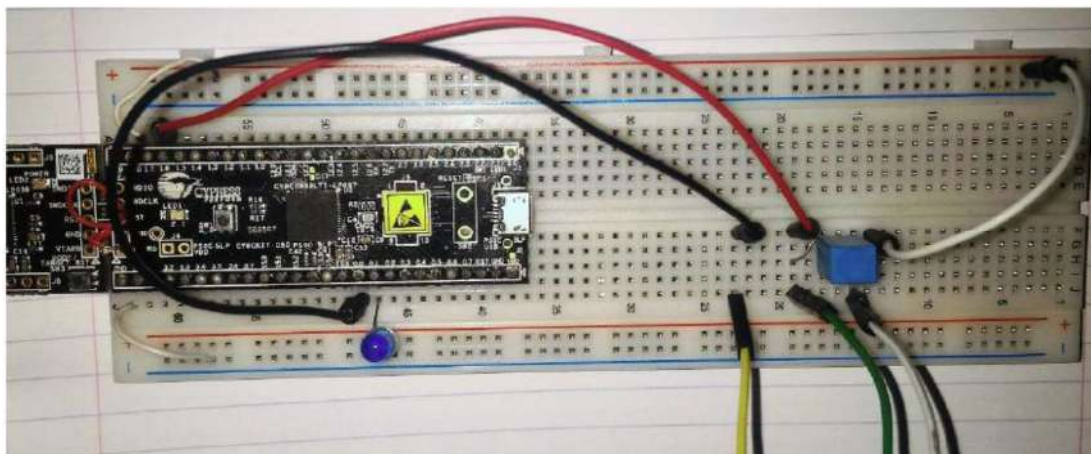
Figure 8: The bread-board integrating the controller-board and the electric circuit.

Author: Marco Machesi.

Table 3: **Experimental Sensors Characteristics**

Substrate	Dimensions	Connection
Glass (sensor 1)	5mm x20mm	Copper wire and silver paint
Thermal release tape (sensor 2)	7mm x 6mm	

particularly semiconductor thin films. An advantage for accurate measurement of low resistance values is the separation of current and voltage electrodes that eliminate the lead and contact existence from the measurement. Because, at this point it is not relevant to know with high accuracy the absolute value of the resistance but it is important to detect with low ratio noise/signal the resistivity variation of the graphene sample, the solution adopted was a simple three cables connection to the sensor (I+, I- and ground), as shown in Figure **7b**. This method is easy to build, gives good results, is portable and cheap.

As we have demonstrated before, graphene was transferred to three substrates, however the experimental tests were made in glass (sensor 1) and plastic film (sensor 2). These features are explained in Table **3**.

The perfect environment to perform the tests on the sensors would be a sealed box where it was possible to introduce specific amounts of CO_2 or other gases, however, in this preliminary stage of the tests, they were performed in an open space (at the laboratory).

In order to analyze the results, the SerialChart application was used. It was connected to the same ComPort of the board and printed a graph of resistance value (blue) and voltage value (red) in real time (Figure **9**). In brown is the current input. The tests were the same for both the sensors. The first step was to measure the resistivity under normal conditions and record their value. A glass bell was then placed on the top of the sensor and checked that no

variations was presented on the resistivity. After that, the presence of CO_2 and H_2O vapor was tested. The tests were performed on different days and in two different laboratories. It was found that, due to the electrical sensitivity of the graphene, the resistivity value changed from one laboratory to the another and from one day to the next due to different atmospheric conditions. All the measurements were made with a current input of 5 µA. This value is high enough for a low noise signal rate and low enough not to degrade the samples. Because of the noise present in the system, values in an estimated range of ±120 Ω were considered.

Tests A and B were done using sensor 2 (graphene on thermal release tape) and test C using sensor 1 (graphene on glass). Table **4** show the sample resistance under normal conditions when the CO_2 bell is applied and with CO_2 and H_2O vapor.

Test A was performed in the first laboratory and the sensor resistance under normal conditions was 9000 (±120) Ω. Applying the glass bell with CO_2, the value decreased immediately and after 15 seconds reached the stable value of 7400 (±120) Ω, representing a decrease of 17,8%. When the bell was removed, it took 4 minutes for the sensor to reach the initial value. Once the initial value was restored, the bell with CO_2 and H_2O vapor was placed, the resistance value started to increase and after 18 seconds reached the stable value of 10900 (±120) Ω. It increased approximately 21%. When the bell was removed, more than 20 min were required to the sensor to reach the initial value.
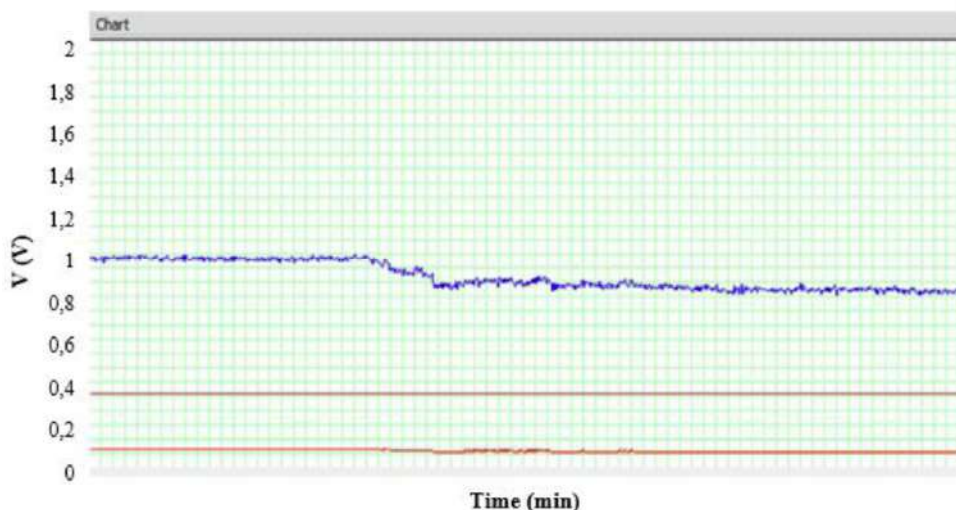
Figure 9: Chart print in the SerialChart program in real time.

Author: Marco Machesi.

Table 4: Comparison between Sample Resistance in Normal Conditions, Applying CO_2 and CO_2 and H_2O Vapor

Test	Resistance (±120 Ω) [Ω]	CO_2 (±120 Ω) [Ω]	CO_2 and H_2O vapor (±120 Ω) [Ω]
A	9000	7400	10900
B	8700	7600	10600
C	3600	3200	4300

Test B was done with the same sensor but in the second laboratory. The sensor resistance in normal conditions was 8700 (±120) Ω. Applying the bell with CO_2 the value was decreasing and reached the normal stable value after 12 seconds. The value decreased by 12,6% to 7600 (±120) Ω. After the bell was removed, approximately 4 min were necessary to the sensor to reach the initial value. When the bell with CO_2 and H_2O vapor was placed, the value started to increase and after 18 seconds it reached the stable value of 10600 (±120) Ω, increasing approximately 22%. Again, when the bell was removed, more than 20 min were necessary to the sensor to reach the initial value.

The last test (test C) was performed again in the first laboratory with sensor A (graphene on glass) with an initial resistance of 3600 (±120) Ω. Applying the bell with CO_2 and after 12 seconds it reached the stable value of 3200 (±120) Ω, decreasing approximately 11%. 3 min after the bell was removed, the sensor reached the initial value. Once the initial value has been restored, the bell with CO_2 and H_2O vapor has been placed and the value increase immediately. After 20 seconds it reached the stable value of 4300 (±120) Ω, an increase of 19,4% After the bell was removed more than 15 minutes were necessary to the sensor to reach the initial value.

CONCLUSION AND FUTURE WORK

With ever-growing environmental concerns, the detection and monitoring of various gaseous species are of critical importance. Indoor air pollutants might be originated from a range of sources. Most of these pollutants, namely CO, CO_2, NO_x, VOCs, PM_{10}, $PM_{2.5}$, relativity humidity and temperature are inhaled and affect human health. That way, the present paper reflects a preliminary study on the importance and the interest of the incorporation of modified graphene in sensors for gas monitoring, air quality and detection of potentially dangerous leaks.

Graphene has significant applications in electronics, presenting itself as a strong candidate in the replacement of silicon in future solid-state devices. However, there are barriers to be transposed, as is the case of the absence of an energy gap (bandwidth energy prohibited). Without the gap, you cannot turn semiconductor devices on and off. In this sense, it is highly desirable to introduce a banned energy band onto graphene in order to shape its transport properties. An adjustable band gap would then be desirable because it

would allow great flexibility in design and optimization of such devices, particularly if such adjustment by applying a variable external electric field.

The results clearly demonstrate that graphene was successfully synthesized and transferred to the substrate and the successfully deposition of Al_2O_3 via ALD on the graphene surface and further demonstrating that the graphene surface functionalization is feasible. An easy way to improve the performance of the sensors presented will be by using insulated cables and better quality connections to reduce the noise present in the system. Although the tests were done in a non-optimal environment with multiple influencing factors and disturbances, it is possible to clearly detect the variations of gases in the air around the sensor, in particular CO_2 and H_2O vapor. These sensors cannot detect small variations of gas particles in the air but they are a starting point for further work toward this goal. From this perspective, a laboratory prototype device based on measuring electrical properties of the sample as a function of the gas absorption is under development. Also, as future work, additional research on the functionalization of graphene will be performed to improve the sensitivity and selectivity of the sensor for air pollutants such as for example VOCs, PM and CO. Finally, it should be noted that a method for the mass production of graphene has not yet been identified being also a future work to be considered.

ACKNOWLEDGEMENTS

REFERENCES

[1] Wei W, Ramalho O, Mandin C. Indoor air quality requirements in green building certifications. Build and Environ 2015; 92: 10-9.
https://doi.org/10.1016/j.buildenv.2015.03.035

[2] Ghebreyesus TA, Al-Ansary LA, Grove JT. World health statistics 2018. World Health Organization; 2018.

[3] Air Quality - Existing Legislation, E. Commission [Internet]. 2017. Available from: http://ec.europa.eu/environment/air/quality/existing_leg.htm

[4] Arroyo P, Lozano J, Suárez JI, Herrero JL, Carmona P. Wireless Sensor Network for Air Quality Monitoring and Control. Chem Eng Trans 2016; 54: 217-22.

[5] Kataoka H, Ohashi Y, Mamiya T, et al. Indoor Air Monitoring of Volatile Organic Compounds and Evaluation of Their Emission from Various Building Materials and Common Products by Gas Chromatography-Mass Spectrometry. In: Advanced Gas Chromatography - Progress in Agricultural Biomedical and Industrial Applications, Dr. Mustafa Ali Mohd, editor. InTech 2010; p 161-84.

[6] Parks H, Needham W, Rajaram S, et al. Semiconductor Manufacturing. In: The electrical engineering Handbook. Electronics, Power Electronics, Optoelectronics, Microwaves, Electromagneticas, and Radar. 3rd ed. Boca Raton: Taylor & Francis Group, LLC 2006; p 64-132.

[7] Xiao Z, Kong LB, Ruan S, et al. Recent Development in Nanocarbon Materials for Gas Sensor Applications. Sens Actuators B Chem 2018; 274: 235-67.
https://doi.org/10.1016/j.snb.2018.07.040

[8] Medvedeva E, Baranov A, Somov A. Design and investigation of thin film nanocomposite electrodes for electrochemical sensors. Sens Actuators B Chem 2016; 236: 858-64.
https://doi.org/10.1016/j.snb.2016.02.104

[9] Hung CM, Thi D, Le T, Hieu N Van. On-chip growth of semiconductor metal oxide nanowires for gas sensors : A review. Journal of Science: Advanced Materials and Devices 2017; 2: 263-85.
https://doi.org/10.1016/j.jsamd.2017.07.009

[10] Ouyang Y, Wang X, Yu G, Song Z, Zhang X. Performance of Amperometric and Potentiometric Hydrogen Sensors. J Mater Sci Technol 2014; 30: 1160-65.
https://doi.org/10.1016/j.jmst.2014.07.001

[11] Li C, Shi G. Carbon nanotube-based fluorescence sensors. J Photochem Photobiol C 2014; 19: 20-34.
https://doi.org/10.1016/j.jphotochemrev.2013.10.005

[12] Barsan N, Koziej D, Weimar U. Metal oxide-based gas sensor research: How to?. Sens Actuators B Chem 2007; 121: 18-35.
https://doi.org/10.1016/j.snb.2006.09.047

[13] Kanan SM, El-kadri OM, Abu-yousef IA, Kanan MC. Semiconducting Metal Oxide Based Sensors for Selective Gas Pollutant Detection. Sensors 2009; 9: 8158-96.
https://doi.org/10.3390/s91008158

[14] Caron A, Redon N, Thevenet F, Hanoune B, Coddeville P. Performances and limitations of electronic gas sensors to investigate an indoor air quality event. Build Environ 2016; 107: 19-28.
https://doi.org/10.1016/j.buildenv.2016.07.006

[15] Ampuero S, Bosset JO. The electronic nose applied to dairy products: A review. Sens Actuators B Chem 2003; 94: 1-12.
https://doi.org/10.1016/S0925-4005(03)00321-6

[16] Atta NF, Galal A, El-Ads EH. Graphene - A Platform for Sensors and Biosensors Applications. In: Biosensors - Micro and Nanoscale Applications. Intech 2015; p 37 - 84.
https://doi.org/10.5772/60676

[17] Jiang W-S, Xin W, Xun S, et al. Reduced graphene oxide-based optical sensor for detecting specific protein. Sens Actuators B Chem 2017; 249: 142-48.
https://doi.org/10.1016/j.snb.2017.03.175

[18] Gutierrez F, Gonzalez-Dominguez JM, Ansón-Casaos A, et al. Single-walled carbon nanotubes covalently functionalized with cysteine: A new alternative for the highly sensitive and selective Cd(II) quantification. Sens Actuators B Chem 2017; 249: 506-14.
https://doi.org/10.1016/j.snb.2017.04.026

[19] Liu CS, Jia R, Ye XJ, Zeng Z. Non-hexagonal symmetry-induced functional T graphene for the detection of carbon monoxide. J Chem Phys 2013; 139: 1-7.
https://doi.org/10.1063/1.4813528

[20] Kumar P, Skouloudis AN, Bell M, et al. Real-time sensors for indoor air monitoring and challenges ahead in deploying them to urban buildings. Sci Total Environ 2016; 560: 150-59.
https://doi.org/10.1016/j.scitotenv.2016.04.032

[21] Mead MI, Popoola OAM, Stewart GB, et al. The use of electrochemical sensors for monitoring urban air quality in low-cost, high-density networks. Atmos Environ 2013; 70: 186-203.
https://doi.org/10.1016/j.atmosenv.2012.11.060

[22] Kumar P, Pirjola L, Ketzel M, Harrison RM. Nanoparticle emissions from 11 non-vehicle exhaust sources - A review. Atmos Environ 2013; 67: 252-77.
https://doi.org/10.1016/j.atmosenv.2012.11.011

[23] Wolkoff P. Indoor air pollutants in office environments: Assessment of comfort, heath, and performance. Int J Hyg Environ Health 2013; 216: 371-94.
https://doi.org/10.1016/j.ijheh.2012.08.001

[24] U.S.EPA. Federal Register:rules and regulations. U.S. Environmental Protection Agency, Air quality index reporting. Fed Regist. 1999; 73: 74932-43.

[25] Kumar P, Morawska L, Martani C, et al. The rise of low-cost sensing for managing air pollution in cities. Environ Int 2015; 75: 199-205.
https://doi.org/10.1016/j.envint.2014.11.019

[26] Capone S, Forleo A, Francioso L, et al. Solid State Gas Sensors: State of the Art and Future Activities. Journal of optoelectronics and Advanced Materials 2004; 5: 1335-348.
https://doi.org/10.1002/chin.200429283

[27] Varghese SS, Lonkar S, Singh KK, Swaminathan S, Abdala A. Recent advances in graphene based gas sensors. Sens Actuators B Chem 2015; 218:160-83.
https://doi.org/10.1016/j.snb.2015.04.062

[28] Justino CIL, Gomes AR, Freitas AC, Duarte AC, Rocha-Santos TAP. Graphene based sensors and biosensors. Trends Analyt Chem 2017; 91: 53-66.
https://doi.org/10.1016/j.trac.2017.04.003

[29] Bollella P, Fusco G, Tortolini C, et al. Beyond graphene: Electrochemical sensors and biosensors for biomarkers detection. Biosens Bioelectron 2017; 89: 152-66.
https://doi.org/10.1016/j.bios.2016.03.068

[30] Wang T, Huang D, Yang Z, et al. A Review on Graphene-Based Gas/Vapor Sensors with Unique Properties and Potential Applications. Nano-Micro Lett 2016; 8: 95-119.
https://doi.org/10.1007/s40820-015-0073-1

[31] Tricoli A, Righettoni M, Teleki A. Semiconductor Gas Sensors: Dry Synthesis and Application. Angew Chem Int Ed Engl 2010; 49: 7632-59.
https://doi.org/10.1002/anie.200903801

[32] Jiménez-Cadena G, Riu J, Rius FX. Gas sensors based on nanostructured materials. Analyst 2007; 132: 1083-99.
https://doi.org/10.1039/b704562j

[33] Chaika AN, Aristov VY, Molodtsova OV. Graphene on cubic-SiC. Prog Mater Sci 2017; 89: 1-30.
https://doi.org/10.1016/j.pmatsci.2017.04.010

[34] He Q, Wu S, Yin Z, Zhang H. Graphene-based electronic sensors. Chem Sci 2012; 3: 1764-72.
https://doi.org/10.1039/c2sc20205k

[35] Kulkarni GS, Reddy K, Zhong Z, Fan X. Graphene nanoelectronic heterodyne sensor for rapid and sensitive vapour detection. Nat Commun 2014; 5: 1-7.
https://doi.org/10.1038/ncomms5376

[36] Ghany NA, Elsherif SA, Handal HT. Revolution of Graphene for different applications: State-of-the-art. Surfaces and Interfaces 2017; 9: 93-106.
https://doi.org/10.1016/j.surfin.2017.08.004

[37] Pumera M, Ambrosi A, Bonanni A, Chng ELK, Poh HL. Graphene for electrochemical sensing and biosensing. Trends Analyt Chem 2010; 29: 954-65.
https://doi.org/10.1016/j.trac.2010.05.011

[38] Kaur G, Gupta S, Dharamvir K. Theoretical investigation of adsorption of gas molecules on Li metal adsorbed at H-site of graphene : A search for graphene based gas sensors. Surfaces and Interfaces 2017; 8: 83-90.
https://doi.org/10.1016/j.surfin.2017.05.002

[39] Schedin F, Geim AK, Morozov SV, et al. Detection of individual gas molecules adsorbed on graphene. Nat Mater 2007; 6: 652-5.
https://doi.org/10.1038/nmat1967

[40] Phiri J, Gane P, Maloney TC. General overview of graphene: Production, properties and application in polymer composites. Mater Sci Eng B Solid State Mater Adv Technol 2017; 215: 9-28.
https://doi.org/10.1016/j.mseb.2016.10.004

[41] Geim AK, Novoselov KS. The rise of graphene. Nat Mater 2007; 6: 183-91.
https://doi.org/10.1038/nmat1849

[42] Chen X, Wu G, Jiang Y, Wang Y, Chen X. Graphene and graphene-based nanomaterials: the promising materials for bright future of electroanalytical chemistry. Analyst 2011; 136: 4631-40.
https://doi.org/10.1039/c1an15661f

[43] Mattevi C, Kim H, Chhowalla M. A review of chemical vapour deposition of graphene on copper. J Mater Chem 2011; 21: 3324-34.
https://doi.org/10.1039/C0JM02126A

[44] Kim KS, Zhao Y, Jang H, *et al*. Large-scale pattern growth of graphene films for stretchable transparent electrodes. Nature 2009; 457: 706-10.
https://doi.org/10.1038/nature07719

[45] Li X, Cai W, An J, Kim S, Nah J, Yang D, *et al*. Large-Area Synthesis of High-Quality and Uniform Graphene Films on Copper Foils. Science 2009; 324: 1312-4.
https://doi.org/10.1126/science.1171245

[46] Nam J, Kim DC, Yun H, *et al*. Chemical vapor deposition of graphene on platinum: Growth and substrate interaction. Carbon N Y 2017; 111: 733-40.
https://doi.org/10.1016/j.carbon.2016.10.048

[47] Geim AK. Graphene: status and prospects. Prospects 2009; 324: 1-8.
https://doi.org/10.1126/science.1158877

[48] Mu W, Fu Y, Sun S, *et al*. Controllable and fast synthesis of bilayer graphene by chemical vapor deposition on copper foil using a cold wall reactor. Chem Eng J 2016; 304: 106-14.
https://doi.org/10.1016/j.cej.2016.05.144

[49] Zhang Y, Chen Y, Zhou K, Liu C. Improving gas sensing properties of graphene by introducing dopants and defects : a first-principles study. Nanotechnology 2009; 20: 1-8.
https://doi.org/10.1088/0957-4484/20/18/185504

[50] Nayak PK, Wang Z, Hedhili MN, Wang QX, Alshareef HN. Semiconductor (CMOS) Device Using a Single-Step Deposition of the Channel Layer. Sci Rep 2014; 4: 1-7.
https://doi.org/10.1038/srep04672

[51] Cadore AR, Mania E, Alencar AB, *et al*. Enhancing the response of NH3 graphene-sensors by using devices with different graphene-substrate distances. Sens Actuators B Chem 2018; 1-19.
https://doi.org/10.1016/j.snb.2018.03.164

[52] Axet MR, Bacsa RR, Machado BF, Serp P. Adsorption on and reactivity of carbon nanotubes and graphene. In: Kadish K, D'souza F, editors. Handbook of Carbon Nano Materials. World Scientific 2014; p. 39-183.
https://doi.org/10.1142/9789814566704_0002

[53] Aroutiounian V. Band Gap Opening in Graphene. Armen J Phys 2013; 6: 141-8.

[54] Varghese SS, Varghese SH, Swaminathan S, Singh KK, Mittal V. Two-Dimensional Materials for Sensing: Graphene and Beyond. Electronics 2015; 4: 651-87.
https://doi.org/10.3390/electronics4030651

[55] Knez M, Nielsch K, Niinistö L. Synthesis and surface engineering of complex nanostructures by atomic layer deposition. Adv Mater 2007; 19: 3425-38.
https://doi.org/10.1002/adma.200700079

[56] Marichy C, Pinna N. Carbon-nanostructures coated/decorated by atomic layer deposition : Growth and applications. Coord Chem Rev 2013; 257: 3232-53.
https://doi.org/10.1016/j.ccr.2013.08.007

[57] George SM. Atomic Layer Deposition : An Overview. Chem Rev 2010; 110: 111- 31.
https://doi.org/10.1021/cr900056b

[58] Elam JW, Groner MD, George SM. Viscous flow reactor with quartz crystal microbalance for thin film growth by atomic layer deposition. Rev Sci Instrum 2013; 73: 2981-7.
https://doi.org/10.1063/1.1490410

[59] Meng X, Byun Y, Kim HS, *et al*. Atomic Layer Deposition of Silicon Nitride Thin Films : A Review of Recent Progress, Challenges, and Outlooks. Materials (Basel) 2016; 9: 1-20.
https://doi.org/10.3390/ma9121007

[60] Kim H, Lee HBR, Maeng WJ. Applications of atomic layer deposition to nanofabrication and emerging nanodevices. Thin Solid Films 2009; 517: 2563-80.
https://doi.org/10.1016/j.tsf.2008.09.007

[61] Neri G, Bonavita A, Rizzo G, *et al*. Towards enhanced performances in gas sensing: SnO2 based nanocrystalline oxides application. Sens Actuators B Chem 2007; 122: 564-71.
https://doi.org/10.1016/j.snb.2006.07.006

[62] Gopel W, Schierbaum K. SNO2 sensors: current status and future prospects. Sens Actuators B Chem. 1995; 27: 1-12.
https://doi.org/10.1016/0925-4005(94)01546-T

[63] Ferrari AC, Basko DM. Raman spectroscopy as a versatile tool for studying the properties of graphene. Nat Nanotechnol 2013; 8: 235-46.
https://doi.org/10.1038/nnano.2013.46

[64] Nayak P, Caraveo-Frescas J, Wang Z, *et al*. Thin Film Complementary Metal Oxide Semiconductor (CMOS) Device Using a Single-Step Deposition of the Channel Layer. Sci Rep 2014; 4: 1-7.
https://doi.org/10.1038/srep04672